WOA-MLSVMs Dirty Degree Identification Method Based on Texture Features of Paper Currency Images

Wei-Zhong Sun, Yue Ma, Zhen-Yu Yin *, Jie-Sheng Wang, Ai Gu, and Fu-Jun Guo

Abstract—**The dirty degree of banknotes determines to some extent whether banknotes can continue to circulate. This paper proposes a whale optimization algorithm based multi-layer support vector machine (WOA-MLSVMs) dirty degree recognition method based on the texture characteristics of banknote images. Based on the contact image sensor to collect the double-sided reflection images of the banknotes under red, green, blue, infrared and ultraviolet light, as well as the transmission images under the green light and infrared light, 22 texture characteristic parameters of the banknotes image based on the gray-scale co-occurrence matrix (GLCM) are extracted to describe the visual characteristics of the banknotes dirty degree, such as energy, entropy and inertia, etc. The banknotes images are selected based on the dirty degree recognition results of MLSVMs to establish the full-spectrum banknote dirty degree recognition sample data set. Five essential dimension estimation methods and seventeen data dimension reduction methods are combined to determine the essential dimension and the optimal dimension reduction method. Finally, WOA-MLSVMs realizes the full-spectrum banknote dirty degree recognition and the simulation results show the effectiveness of the proposed strategy.**

Index Terms—**banknote dirty degree, texture features, whale optimization algorithm, data dimension reduction, support vector machine**

Manuscript received February 4, 2021; revised May 20, 2021. This work was supported by the First Batch Major Science and Technology Platform Opening Projects of Institution of Higher Learning of Liaoning Province (Grant No. USTLGXZD201902).

Wei-Zhong Sun is a doctoral candidate of University of Chinese Academy of Sciences, Beijing, 100049, P. R. China, Shenyang Institute of Computing Technology, Chinese Academy of Sciences, Shenyang, 110168, P. R. China, and a lecturer of School of Computer Science and Software Engineering, University of Science and Technology Liaoning, Anshan, 114051, P. R. China. (e-mail: weizhongsun@126.com).

Yue Ma is a research fellow of University of Chinese Academy of Sciences, Beijing, 100049, P. R. China and Shenyang Institute of Computing Technology, Chinese Academy of Sciences, Shenyang, 110168, P. R. China. (e-mail: mayue@sict.ac.cn).

Zhen-Yu Yin is a research fellow of University of Chinese Academy of Sciences, Beijing, 100049, P. R. China and Shenyang Institute of Computing Technology, Chinese Academy of Sciences, Shenyang, 110168, P. R. China. (Corresponding author, e-mail: congmy@163.com).

Jie-Sheng Wang is a professor of School of Electronic and Information Engineering, University of Science and Technology Liaoning, Anshan, 114051, P. R. China. (Corresponding author, phone: 86-0412-2538246; fax: 86-0412-2538244; e-mail: wang_jiesheng@126.com).

Ai Gu is a doctoral candidate of University of Chinese Academy of Sciences, Beijing, 100049, P. R. China and Shenyang Institute of Computing Technology, Chinese Academy of Sciences, Shenyang, 110168, P. R. China. (e-mail: guai14@mails.ucas.edu.cn).

Fu-Jun Guo is a postgraduate student of School of Electronic and Information Engineering, University of Science and Technology Liaoning, Anshan, 114051, P. R. China. (e-mail: 1468239974@qq.com).

I. INTRODUCTION

With the development of the commodity economy, currency emerged as a general equivalent to measure the value of commodities. Currency not only has functions such as value scale and means of circulation, but also has the functions of regulating the social economy and promoting the development of the national economy. Paper currency is a mandatory value symbol issued by the state to replace metal currency as a means of circulation. At present, banknotes, as a form of currency commonly used by all countries in the world, play a pivotal role in all countries in the world. As a medium of commodity circulation, the circulation of paper money is increasing day by day. The proportion of defective and dirty banknotes has also become larger and larger with the increase of circulation time, which will affect the convenience of people's lives and commodity transactions to varying degrees. Therefore, when the paper currency reaches a certain degree of contamination, the bank will often recover and destroy it collectively. Banks and other financial institutions often use financial equipment, such as banknote sorting machines, to recognize the face value, authenticity, and serial number of banknotes through image processing, pattern recognition and other technologies.

Scholars at home and abroad have also conducted a certain degree of research on the recognition of banknote characteristics. Ji et al. [1] discussed the four main research areas of various sensors in the field of accurate banknote recognition (banknote recognition, counterfeit banknote detection, serial number recognition, and fitness classification), and discussed the advantages and disadvantages of the methods proposed in these studies. Zhang et al. [2] proposed a multi-feature fusion banknote authenticity recognition method based on the combination of D-S evidence theory and support vector machine, which solved the low accuracy and low stability problems of single-feature banknote authenticity recognition. Yeh et al. [3] proposed a counterfeit banknote recognition system based on a multi-core support vector machine that minimizes the false alarm rate. Simulation results show that this method is superior to single-core support vector machines, standard support vector machines and multi-SVM classifiers. Takeda et al. [4] proposed a new banknote recognition system based on neural network (NN), which uses the mask-based small-scale neural recognition technology and genetic algorithm (GA)-based mask optimization technology, and digital signal processor (DSP) neural hardware technology. Oyedotun et al. [5] proposed three cognitive hypothetical frameworks for visual recognition of banknote

denominations based on competitive neural networks. Pham et al. [6] aimed at the characteristics that some areas of banknotes are easier to distinguish in the type, side and direction of the banknote than other areas, and proposed a method that uses a one-dimensional visible light sensor to collect images, and selects more distinguishable areas on the basis of similar mapping to identify banknotes. The experimental results of different types of banknote databases show that this method is better than previous methods. Lin et al. [7] attributed the signal-to-noise ratio to a sequence prediction problem and proposed a banknote serial number recognition (SNR) method based on deep learning. The improved convolutional neural network was used to extract the input image feature sequence, which is used as the input of the bidirectional recurrent neural network (BRNNs), and finally the output of the BRNNs is decoded by the connection time classification to realize label recognition. Jin et al. [8] established a novel banknote image processing system, including banknote recognition, general wear assessment and feature recognition, and proposed a banknote image registration algorithm based on free deformation model (FFD), which improved the processing capacity of low-quality banknotes greatly and reduced the false detection rate. Han et al. [9] studied the joint paper currency type recognition and counterfeit currency detection method based on machine learning, and proposed an interpretative artificial intelligence method to visualize the recognition and detection area, which is better than the traditional method. The serial method has significantly improved the calculation time. Choi et al. [10] studied a fast banknote serial number recognition method based on machine learning, which can recognize multiple digital serial numbers at the same time, and can automatically detect the serial number interest area from the input image. It also adopts a simplified deep learning model and the Bayesian optimization method is used for classification, which significantly improves the classification performance of banknotes. Pham et al. [11] proposed a multinational banknote classification method based on visible light images by using a one-dimensional line sensor to collect visible light images and combine the information of each denomination and convolutional neural network (CNN) to realize the classification. Experiments results on the six national banknote image database of 62 denominations show that the classification accuracy of this algorithm is 100%. In order to improve the accuracy of defect detection in banknote classification, Gai et al. [12-13] proposed a new banknote image crack and scratch detection algorithm, which used four-layer wavelet transform and least square method to register banknote images. The Kirsch operator is used to detect the edge information, and the defect features that are robust to grayscale changes are constructed.

However, no matter at home or abroad, few scholars have conducted research on the recognition of the dirty degree of banknotes [1]. The specific reasons are as follows. First of all, the dirtiness of banknotes is a relatively subjective concept. Different people have different understandings of the banknotes dirty degree. The dirtiness characteristics of banknotes are also a relatively complex indicator, and there is a lack of commonly recognized evaluation standards in the financial industry. Secondly, financial equipment is relatively fast in counting banknotes, so it has high requirements on data collection speed, machine calculation speed and image recognition algorithms. Finally, it is very difficult to unify the stability and consistency of banknote recognition results, as well as to conform to the visual laws of the human eye and human subjective identification. How to reasonably solve the above problems has become the focus of research by relevant personnel. The dirty degree characteristics of banknotes can be expressed in terms of optical characteristics, hardness, weight, and roughness. Among above features, the optical features can most intuitively reflect the dirty degree of banknotes [14].

Therefore, financial devices such as banknote sorters usually use optical image sensors to collect the optical characteristics of banknotes to complete banknote recognition. The Bank of Netherlands has conducted a lot of research on the dirty degree recognition of banknotes [15]. The research shows that the dirtiness of banknotes mainly come from the stains remaining after the human fingers touch them. This stain is mainly reflected in yellow or brown, Under the dark blue or indigo spectrum, the difference between banknotes with different dirty grades is the biggest. Kwon et al. [16] used visible light reflection images and infrared light transmission images to identify banknote dirtiness, and believed that visible light reflection images and infrared light transmission images have a great influence on the classification of banknotes.

In this paper, a WOA-MLSVMs dirty degree recognition method was proposed based on the texture characteristics of banknote images. The banknotes images with different levels of dirty degree under various light sources are collected, and 22 texture characteristic parameters are extracted based on the gray-scale co-occurrence matrix to describe the visual characteristics of the banknotes dirtiness, such as energy, entropy and inertia, etc. Five essential dimension estimation methods and seventeen data dimension reduction methods are combined to determine the essential dimension and optimal dimension reduction method. Finally, the WOA-based MLSVMs is used to realize the full-spectrum banknotes dirty degree recognition, and simulation results show the effectiveness of the proposed method.

II. Dirty Degree Analysis of Banknote Images Texture Feature Extraction

A. Image Collection of Banknotes Based on CIS Sensor

Before collecting images, it is necessary to prepare banknotes and manually sort the banknotes. This article divides 1000 banknotes into five categories according to their dirtiness: New, Clean, Normal, Dirty and Very Dirty, whose number is 272 sheets, 200 sheets, 220 sheets, 170 sheets and 138 sheets, individually [17]. Then the contact image sensor is used to collect 10 double-sided reflection images of these five types of banknotes under red light, green light, blue light, infrared light, and ultraviolet light, and the 2 transmission images under green light and infrared light, which are used to identify the dirtiness of banknotes. The captured images are segmented from the background and revised to achieve the same size of pixels, where the resolution of each image is 600×288 pixels. Fig. 1 shows the reflected images and transmission images of 100 yuan.

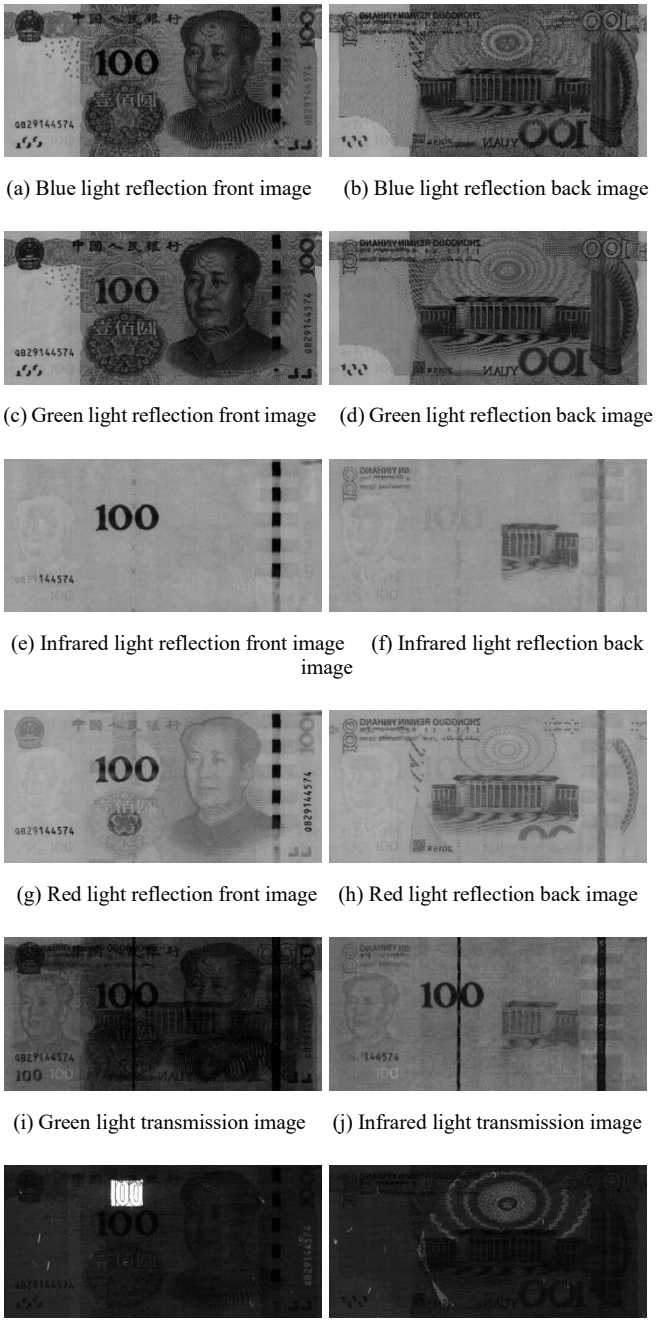

(a) Blue light reflection front image (b) Blue light reflection back image

(c) Green light reflection front image (d) Green light reflection back image

(e) Infrared light reflection front image (f) Infrared light reflection back image

(g) Red light reflection front image (h) Red light reflection back image

(i) Green light transmission image (j) Infrared light transmission image

(k) UV light reflection front image (l) UV light reflection back image

Fig. 1 Images of banknotes.

B. Texture Feature Extraction of Banknote Images Based on Gray Level Co-occurrence Matrix

The texture is a pattern with small shapes and regularly arranged in a certain range of the image. The image textures can reflect the dirty characteristics of the banknote image. The gray level co-occurrence matrix (GLCM) reflects the characteristic relationship of the gray level in the image with respect to the direction, the adjacent interval, and the amplitude of change. It is based on the estimated second-order combination conditional probability density function of the image. Fig. 2 is a schematic diagram of the gray-level co-occurrence matrix, where, i and j represent the gray value of the corresponding pixel [18]. Let $f(x,y)$ be a two-dimensional digital image, and GLCM refers to the pixels whose gray level is i in the image $f(x,y)$, and probability $P(i,j,\delta,\theta)$ that appears at the same time with the deflection angle θ, the distance δ, and the pixel $(x+\Delta x, y+\Delta y)$ with the value j. 22 texture feature parameters based on GLCM, such as angular second moment, entropy, dissimilarity, and contrast, are used to describe the texture features of banknote images. This article divides the banknotes according to dirty degree into five categories: New, Clean, Normal, Dirty and Very dirty. Taking a "very new" banknote as an example, the 12 images, which are the blue light front and back reflection images, green front and back reflection images, infrared front and back reflection images, red light front and back reflection images, green light transmission images, infrared light transmission images, and UV front and back reflection images, are adopted to extract the $22\times12=264$ texture features so as to obtain the samples data set, which are shown in Table 1 and Table 2.

C. Analysis of Texture Characteristics of Banknote Images

The dirty degree characteristics of banknotes can be expressed in terms of optical characteristics, hardness, weight, and roughness. Among the above features, the optical feature can most intuitively reflect the dirty features of the banknote. Therefore, financial devices such as banknote sorters usually adopt the optical image sensors to collect the optical characteristics of banknotes to complete banknote recognition. However, banknote images and their texture characteristics collected based on different light sources have different effects on the recognition of banknotes' dirtiness. Therefore, the obtained 22 banknotes texture features are analyzed, part of whose results are shown in Fig. 3(a)-(d). Banknotes with different dirty degree are divides into five categories: New, Clean, Normal, Dirty, and Very dirty, with 272 sheets, 200 sheets, 220 sheets, 170 sheets and 138 sheets, respectively. A total of 12 banknote images are collected by the CIS image sensor, which include the front and back reflection images under blue light, green light, infrared light, red light and UV light, transmission images under green light and infrared light. Then 22 texture features of these 12 images for all 5 types of banknotes are averaged for statistical analysis. It can be seen from Fig. 3 that the texture features of banknote images based on the gray-level co-occurrence matrix can reflect the dirty degree of banknotes, but the different texture characteristics of banknotes under different light sources have different effects on the recognition of banknote dirtiness. Generally speaking, the texture characteristics under the red light front and back reflection images, the ultraviolet light front and back reflection image have no obvious effect on the recognition of the banknotes dirty degree.

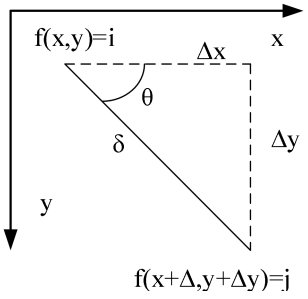

Fig. 2 Gray-level co-occurrence matrix.

TABLE 1 DATA SAMPLES BASED ON GLCM-BASED TEXTURE FEATURES (1)

Serial number	Texture feature	Blue light reflection front image	Blue light reflection back image	Green light reflection front image	Green light reflection back image	Infrared light reflection front image	Infrared light reflection back image
1	Autoc	13.361	12.293	11.929	12.361	25.932	24.658
2	Contr	0.650	0.744	0.913	1.007	0.200	0.142
3	Corrm	0.862	0.806	0.818	0.735	0.838	0.746
4	Corrp	0.862	0.806	0.818	0.735	0.838	0.746
5	Cprom	169.596	112.070	185.124	103.063	100.909	8.438
6	Cshad	9.444	4.803	12.373	2.741	-12.188	-1.787
7	Dissi	0.469	0.527	0.600	0.653	0.173	0.135
8	Energ	0.081	0.076	0.067	0.064	0.520	0.596
9	Entro	2.760	2.820	2.904	2.951	1.127	1.029
10	Homom	0.791	0.768	0.745	0.724	0.917	0.934
11	Homop	0.783	0.758	0.731	0.708	0.916	0.933
12	Maxpr	0.127	0.150	0.111	0.109	0.7060	0.767
13	Sosvh	13.578	12.563	12.285	12.761	25.876	24.576
14	Savgh	6.730	6.558	6.285	6.622	10.083	9.889
15	Svarh	28.579	25.176	24.969	25.357	84.761	81.351
16	Senth	2.283	2.284	2.305	2.291	1.000	0.924
17	Dvarh	0.650	0.744	0.913	1.007	0.200	0.142
18	Denth	0.875	0.926	1.001	1.038	0.481	0.405
19	Inf1h	-0.405	-0.338	-0.340	-0.263	-0.372	-0.426
20	Inf2h	0.868	0.826	0.834	0.769	0.634	0.654
21	Indnc	0.950	0.944	0.937	0.931	0.981	0.985
22	Idmnc	0.990	0.989	0.987	0.985	0.997	0.998

TABLE 2 DATA SAMPLES BASED ON GLCM-BASED TEXTURE FEATURES (2)

Serial number	Texture feature	Red light reflection front image	Red light reflection back image	Green light transmission image	Infrared light transmission image	UV light reflection front image	UV light reflection back image
1	Autoc	24.731	25.345	4.12	14.554	2.753	2.109
2	Contr	0.390	0.407	0.224	0.159	0.198	0.239
3	Corrm	0.781	0.721	0.866	0.845	0.882	0.612
4	Corrp	0.781	0.721	0.866	0.845	0.882	0.612
5	Cprom	70.929	21.459	26.575	36.807	375.900	4.806
6	Cshad	-8.396	-3.300	4.624	-6.828	29.626	1.187
7	Dissi	0.298	0.337	0.214	0.146	0.145	0.218
8	Energ	0.219	0.217	0.229	0.556	0.440	0.374
9	Entro	1.961	1.973	1.797	1.156	1.128	1.307
10	Homom	0.862	0.842	0.895	0.929	0.933	0.894
11	Homop	0.860	0.838	0.894	0.929	0.932	0.893
12	Maxpr	0.393	0.399	0.380	0.739	0.611	0.554
13	Sosvh	24.773	25.394	4.181	14.514	2.808	2.184
14	Savgh	9.806	9.964	3.686	7.515	2.838	2.772
15	Svarh	68.719	71.255	7.362	43.84	6.457	3.679
16	Senth	1.709	1.672	1.626	1.039	1.022	1.133
17	Dvarh	0.390	0.407	0.224	0.159	0.198	0.239
18	Denth	0.665	0.720	0.536	0.428	0.424	0.548
19	Inf1h	-0.382	-0.311	-0.500	-0.437	-0.453	-0.275
20	Inf2h	0.777	0.719	0.835	0.690	0.695	0.584
21	Indnc	0.968	0.963	0.976	0.984	0.984	0.976
22	Idmnc	0.994	0.994	0.997	0.998	0.997	0.996

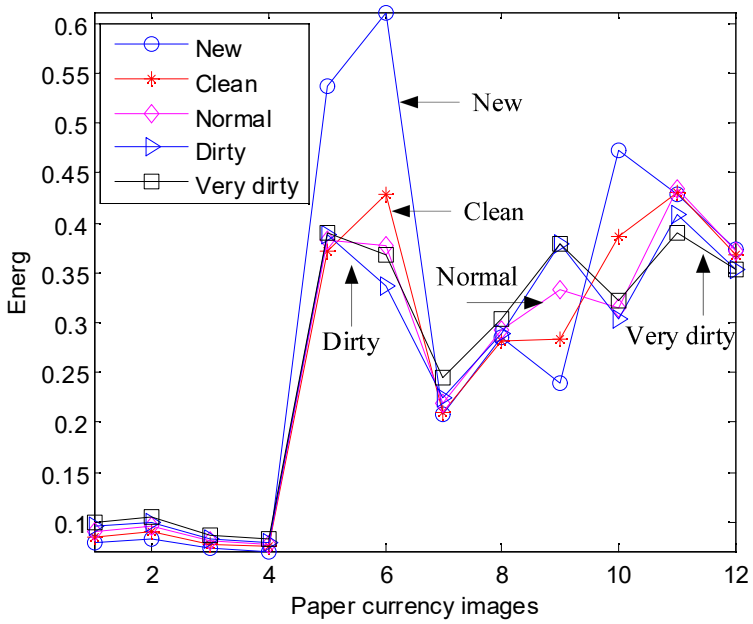

(a) Energ

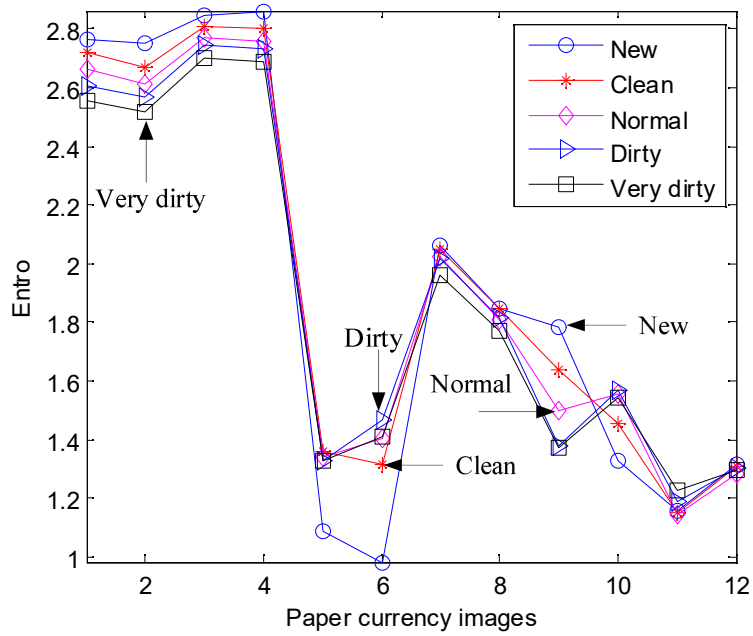

(b) Entro

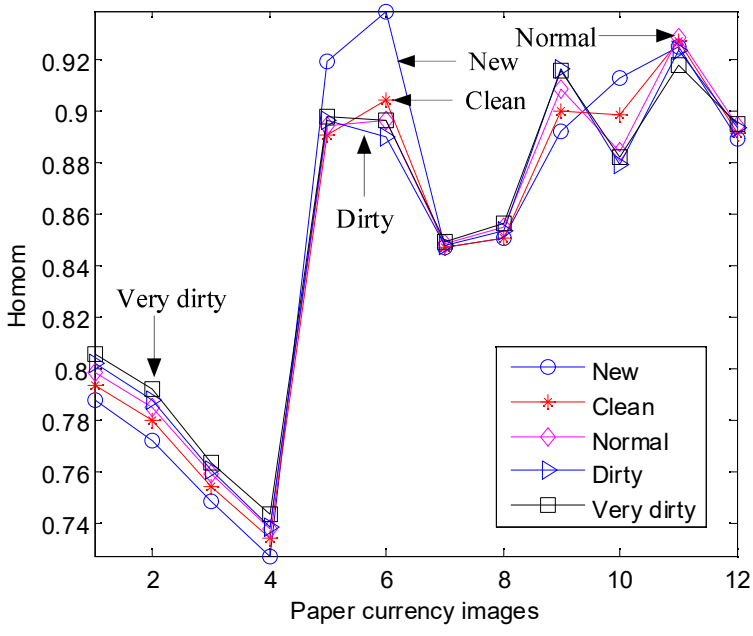

(c) Homom

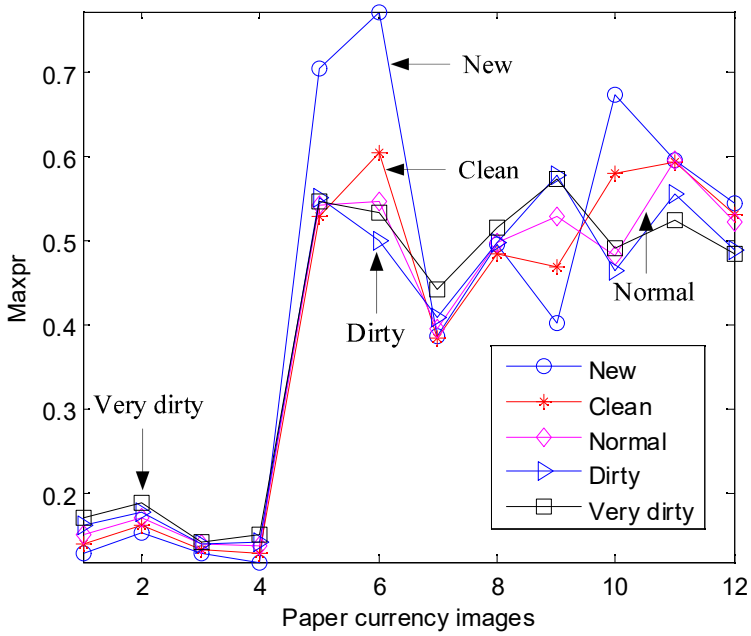

(d) Maxpr

Fig. 3 Paper currency texture characteristics based on different spectra.

It can be seen from Fig. 3 that the texture features of banknotes images under different light sources have inconsistent effects on the recognition of banknotes' dirtiness. Generally speaking, based on the red light front and back reflection images and ultraviolet front and back reflection images, the texture characteristics of the banknotes are not effective in recognizing the dirtiness of banknotes. So the texture features data of 4 images under red light front and back reflection and ultraviolet front and back reflection are removed, and the banknote dirty degree recognition system is established with 176 texture features of other 8 banknotes images. The essential dimension analysis and the selection of dimension reduction methods are carried out. Then the whale optimization algorithm (WOA) is adopted to optimize the parameters of MLSVMs.

III. Essential Dimension Estimation and Dimension Reduction of High-dimensional Feature Data

A. Estimation of Essential Dimension

Through the extraction and analysis of texture features of banknotes under full spectrum, texture features of 4 images under red light front and back reflection and ultraviolet front and back reflection are eliminated, and the banknotes dirty degree identification sample database is established with 176 texture features of other 8 images. But 176-dimensional features will increase computational complexity and storage space, and there will inevitably be a lot of redundant information. Therefore, it is necessary to carry out essential dimensional analysis and data dimension reduction to better highlight the hidden relationship and law among the high-dimensional data, that is to say that the determination of the "essential" dimension of the low-dimensional structure hidden in the high-dimensional data is an important key to dimension reduction.

Suppose there are n samples in the high-dimensional space R^p, represented by $X_1, X_2, \cdots, X_n$, and in the low-dimensional space $R^m (m << p)$, represented by $Y_1, Y_2, \cdots, Y_n$. The mapping from high-dimensional space to low-dimensional space can be expressed as $X_i = g(Y_i)$, where $i = 1, 2, \cdots, n$, and m is the essential dimension. Scholars at home and abroad have proposed many essential dimension estimation methods, such as the correlation dimension estimator, the maximum likelihood estimator, and the geodesic minimum spanning tree algorithm [19-20]. In order to reduce the dimension of the input variables of the multi-layer support vector machines (MLSVMs) in the recognition method of banknotes dirty degree, and to avoid its unstable influence on the output results, this paper also adopts five essential dimension estimation methods, the correlation dimension (CD), nearest neighbor dimension (NND), geodesic minimum spanning tree (GMST), principal component analysis (PCA), and maximum likelihood estimator (MLE), to realize the essential dimension estimation of the banknotes dirty degree data set. This data set is composed of texture features under blue light front and back reflection images, green front and back reflection images, infrared front and back reflection images, green light transmission image, infrared light transmission image and full spectrum image. The estimation results are shown in Table 3.

The NND estimator has the essential dimension of the texture features under all light sources is 1. The PCA method is used for the texture features of blue front reflection images, infrared front and back reflection images, green light transmission images and infrared light transmission images and the essential dimension of the data is 1, and the estimation results are slightly different under other light sources. The essential dimension estimation results of 176 high-dimensional data for full spectrum images under CD estimator, GMST algorithm, PCA method, and MLE are 2, 9, 5, and 7. So 17 data dimension reduction methods will be used to reduce the dimension of high-dimensional features data in these four dimensions.

TABLE 3 ESTIMATION RESULTS OF ESSENTIAL DIMENSIONS

Data	Data dimension	Essential dimension estimation method				
		CD	NND	GMST	PCA	MLE
Blue light reflection front image	22	3	1	5	1	4
Blue light reflection back image	22	2	1	4	2	4
Green light reflection front image	22	3	1	4	2	4
Green light reflection back image	22	2	1	4	3	4
Infrared light reflection front image	22	2	1	3	1	3
Infrared light reflection back image	22	2	1	4	1	3
Green light transmission image	22	2	1	4	1	3
Infrared light transmission image	22	2	1	3	1	3
Full spectrum image	176	2	1	9	5	7

B. Dimension Reduction of High-dimensional Feature Data

Based on the 176-dimensional texture features of the banknotes full-spectrum images and the multi-level support vector machines (MLSVMs) for banknotes dirty degree recognition, the input vector dimension is too large, which will make the network topology large and the training complex, and there may be differences between various variables redundancy, which will interfere with the classification process, so it is necessary to reduce the dimension of high-dimensional data information. Four essential dimension estimators including correlation dimension estimator, geodesic minimum spanning tree algorithm, principal component analysis method and maximum likelihood estimator, are used to obtain the essence of the full spectrum 176-dimensional texture feature high-dimensional data, and the dimensional estimation results are 2, 9, 5, and 7. Then 17 data dimension reduction methods are used to carry out the dimension reduction on the 176-dimensional texture features under four dimensions (2, 5, 7 and 9), which are principal component analysis (PCA), multidimensional scaling (MDS), probabilistic PCA (ProbPCA), factor analysis (FA), gaussian process latent variable model (GPLVM), Laplacian eigenmaps (Laplacian), landmark isomap, diffusion maps (DM), kernel principal component analysis (Kernel PCA, KPCA), stochastic neighbor embedding (SNE), symmetric stochastic neighbor embedding (SymSNE), t-distributed stochastic neighbor embedding (tSNE), locality preserving projection (LPP), neighborhood preserving embedding (NPE), linear local tangent space alignment (LLTSA), stochastic proximity embedding (SPE) and deep autoencoders (DA). Then the radial basis function-based MLSVMs is used to recognize the banknotes dirty degree on the dimension reduced data. The simulation results are listed in Table 4. It can be seen from Table 4 that the results of using MLSVMs based on radial basis function to recognize the banknotes dirty degree with different dimension reduction data are very different, only two data dimension reduction strategies (Laplacian eigenmaps and t-distributed stochastic neighbor embedding) have an accuracy rate of greater than 51%, with the highest recognition rates reaching 57% and 54% respectively. In addition, only the recognition rate by using the diffusion maps (DM) as the data dimension reduction strategy under the dimension 2 reaches 51%. Therefore, this paper finally uses these two data dimension reduction strategies to dispose the 176-dimensional texture feature high-dimensional data of the full-spectrum images, which can reduce the dimension of the input vector of MLSVMs, simplify the network topology and remove redundancy between variables.

IV. MLSVMS RECOGNITION METHOD OF BANKNOTES DIRTY DEGREE BASED ON WOA

A. Support Vector Machine

Support vector machine (SVM) is a classification model. Its main idea is to use the method of minimizing structural risk to construct a better hyperplane to ensure that the separation distance between the sample points on both sides of the hyperplane and the hyperplane is maximized [21].

TABLE 4 RECOGNITION RESULTS OF MLSVMS BASED ON DIFFERENT DIMENSION REDUCTION METHODS

Data dimension reduction method	Accuracy rate of banknote dirt degree recognition (%)			
	Dim=2	Dim=5	Dim=7	Dim=9
Principal component analysis（PCA）	42	42	37	42
Multi-dimensional metric（MDS）	42	42	37	42
Probabilistic principal component analysis（ProbPCA）	31	20	29	22
Factor analysis（FA)	41	28	28	28
Gaussian process hidden variable model（GPLVM）	42	41	37	42
Laplace feature map（Laplacian)	**57**	**53**	**55**	**53**
Landmark isometric feature mapping Landmark isometric feature mapping（Landmark Isomap）	20	20	20	20
Extended mapping（DM）	51	49	43	40
Nuclear principal component analysis（KPCA）	20	20	20	20
Random neighborhood embedding（SNE）	20	20	20	20
Symmetric random neighborhood embedding（SymSNE）	20	20	20	20
t-distributed random neighborhood embedding（tSNE）	**54**	**54**	**54**	**52**
Locally preserved projection（LPP）	20	20	20	20
Neighborhood keep embedded（NPE）	36	38	36	35
Linear local tangent space arrangement（LLTSA）	20	20	20	20
Locally preserved projection（SPE）	31	30	31	20
Deep autoencoder（DA）	20	20	36	20

When a sample set space $\Omega=\{(x_i,y_i)|i=1,2,\cdots,n\}$, $x_i\in R, y_i\in R$ is given to train the classification model $f(x)$, the model is then used to classify the test sample set, the consistency of the prediction result category and the test data category are compared, and the accuracy rate is calculated to obtain the final result. In the SVM classifier, the existing hyperplane H can be expressed as:

$$w\cdot x+b=0 \tag{1}$$

Eq. (1) makes:

$$\begin{aligned} x_i\cdot w+b\geq+1,\ y_i=+1\\ x_i\cdot w+b\leq-1,\ y_i=-1 \end{aligned} \tag{2}$$

where, w is the normal vector of H, which determines the direction of the hyperplane; x is the feature vector, and b is a real offset to determine the distance between the hyperplane and the origin. Based on Eq. (1) and (2), obtain:

$$y_i(x_i\cdot w+b)-1\geq 0,\ \forall i \tag{3}$$

According to Eq. (1) and (3), when w and b change in the same ratio, the H defined by them remains unchanged. In order to eliminate this problem, H and $\{w,b\}$ can be mapped to each other, and the following restriction must be applied on w and b.

$$\min_i|x_i\cdot w+b|=1,\ i=1,2,\cdots,l \tag{4}$$

Assuming that the shortest distance from the sample in category $+1$ to H is D_+, the shortest distance from the sample in category -1 to H is D_-, then the edge of H is D_++D_-. When the two samples are of equal importance, the ideal H should satisfy $D_+=D_-$. At this time, the edge of H is defined by hyperplane $H_1: w\cdot x+b=1$ and $H_2: w\cdot x+b=-1$, and there is a parallel relationship between these two hyperplane and H. It can be seen from Eq. (3) that all training samples are not in H_1 and H_2. As a result, the working principle of SVM can be transformed into the following optimization problem.

$$\min_{w,b}=\frac{1}{2}\|w\|^2 \tag{5}$$

Introduce the Lagrange multiplier α_i to obtain:

$$\begin{aligned} &\min_{w,b}L_p=\frac{1}{2}\|w\|^2-\sum_{i=1}^{l}\alpha_i y_i(x_i\cdot w+b)+\sum_{i=1}^{l}\alpha_i\\ &s.t.\begin{cases}\dfrac{\partial L_p}{\partial\alpha}=0\\ \alpha_i\geq 0,\ \forall i\end{cases} \end{aligned} \tag{6}$$

$$\begin{aligned} &\max_{\alpha}L_D=\frac{1}{2}\|w\|^2-\sum_{i=1}^{l}\alpha_i y_i(x_i\cdot w+b)+\sum_{i=1}^{l}\alpha_i\\ &s.t.\begin{cases}\dfrac{\partial L_D}{\partial w}=0\\ \dfrac{\partial L_D}{\partial b}=0\\ \partial_i\geq 0,\ \forall i\end{cases} \end{aligned} \tag{7}$$

Further rewrite the constraints in Eq. (7) to obtain:

$$w=\sum_{i=1}^{l}\alpha_i y_i x_i \tag{8}$$

$$\sum_{i=1}^{l}\alpha_i y_i=0 \tag{9}$$

Substitute Eq. (8) and (9) into Eq. (7) to get the final form of SVM model described as follows.

$$\begin{aligned} &\max_{\alpha}L_D=\sum_{i=1}^{l}\alpha_i-\frac{1}{2}\sum_{i=1}^{l}\sum_{j=1}^{l}\alpha_i\alpha_j y_i y_j(x_i\cdot x_j)\\ &s.t.\begin{cases}\displaystyle\sum_{i=1}^{l}\alpha_i y_i=0\\ \alpha_i\geq 0,\ \forall i\end{cases} \end{aligned} \tag{10}$$

After Eq. (10) is solved by quadratic programming to obtain the optimal solution $a^*=[a_1^*,a_2^*,.....,a_l^*]^T$, according to Eq. (8), the optimal w^* and b^* corresponding to H can be calculated.

$$\begin{cases} w^*=\displaystyle\sum_{i=1}^{l}a_i^*x_i y_i\\ b^*=-\dfrac{1}{2}w^*(x_r+x_s)\end{cases} \tag{11}$$

where, x_r and x_s are any pair of support vectors in two categories. The final optimal classification function can be described as:

$$f(x)=\mathrm{sgn}\left[\sum_{i=1}^{l}a_i^*y_i(xx_i)+b\right] \tag{12}$$

For nonlinear (linear inseparable) problems, the input space can be mapped to a high-dimensional feature space through appropriate nonlinear transformations, and then the optimal function is constructed in this space to minimize the defined risk function. According to Mercer's theorem, there is a mapping φ and kernel function $K(x_i,x_i)$ to satisfy $K(x_i,x_i)=\phi(x_i)\cdot\phi(x_i)$. Then the optimal classification surface is found in the high-dimensional space Z. That is to say that the optimal classification function is determined by selecting the appropriate kernel function and calculating the parameters to maximize the objective function. If it is still inseparable in a high-dimensional space, SVM classifies by introducing a standard C-support vector machine (C-SVM) with a nonlinear soft interval of slack variables and penalty factors, allowing the classifier to have certain classification errors (soft interval) [22]. In order to enhance the promotion ability, the concept of the soft edge optimal hyperplane is introduced, that is to say that the non-negative variable $\xi_i\geq 0$ is introduced, and the constraint conditions are relaxed as:

$$y_i(w\cdot x_i+b)-1+\xi_i\geq 0 \tag{13}$$

Minimizing $\sum_{i=1}^{n}\xi_i$ can minimize the mis-classification sample, then the optimization problem can be expressed as:

$$\begin{aligned} &\min(\frac{1}{2}\|w\|^2+C\sum_{i=1}^{n}\xi_i)\\ &s.t\ \ y_i(w\cdot x_i+b)-1+\xi_i\geq 0\ \ (i=1,2,...,n)\\ &\xi_i\geq 0 \end{aligned} \tag{14}$$

where, $\xi_i \geqslant 0$ is a slack variable, and C is a penalty factor that comprehensively considers the least mis-classification samples and the maximum classification interval. According to the Lagrange method, the original problem is transformed into a dual problem for solution, namely:

$$\begin{aligned} &\max \sum_i \alpha_i - \frac{1}{2}\sum_{i,j} \alpha_i \alpha_j y_i y_j K(x_i, x_j) \\ &s.t \qquad \sum_i \alpha_i y_i = 0 \\ &\qquad 0 \le \alpha_i \le C \end{aligned} \tag{15}$$

The corresponding discriminant function Eq. (12) can be converted to:

$$f(x) = \operatorname{sgn}(\sum_i \alpha_i y_i K(x_i, x) - b) \tag{16}$$

At present, the more commonly used inner product kernel functions (kernel functions) mainly include polynomial function (PF), radial basis function (RBF) and Sigmoid function. Different kernel functions correspond to different support vectors. Among them, RBF function used in this paper is shown in Eq. (17).

$$K(x_i, x) = \exp\{-\frac{|x_i - x|^2}{\gamma^2}\} \tag{17}$$

where, x is the input vector, x_i is the support vector ($i = 1, \cdots, s$), s is the number of support vectors, and γ is the width of the kernel function.

B. Whale Optimization Algorithm

Whale Optimization Algorithm (WOA) is an algorithm based on swarm intelligence proposed by Seyedali Mirjalili and Andrew Lewis in 2016 based on the hunting behavior of humpback whales [23]. WOA establishes a mathematical model to solve the optimization problems by simulating the predation behavior of whale populations in the sea. In order to convert the predation process of whales into a mathematical model, WOA regards the optimal value in the searching space as prey in the ocean. The search agent continuously explores the searching space through the location update mechanism, and finally moves closer to the area where the optimal value is located. In order to further simulate the predation process of whales, WOA designed two mathematical models, namely the shrinking enveloping mechanism and the spiral updating mechanism, and it is assumed that the probability of using these two models is equal [24-25]. In order to realize this mathematical model, the algorithm firstly generates a random number p between [0,1]. If it is $p < 0.5$, the shrinking encircling mechanism is selected and if $p \geq 0.5$, the spiral updating mechanism is selected, which is described as follows.

$$\vec{X}(t+1) = \begin{cases} \vec{X}_P(t) - \vec{A} \cdot \left| \vec{C} \cdot \vec{X}_P(t) - \vec{X}(t) \right| & if \quad p < 0.5 \\ \vec{D} \cdot e^{bl} \cdot \cos(2\pi l) + \vec{X}_P(t) & if \quad p \geq 0.5 \end{cases} \tag{18}$$

The shrinking enveloping mechanism can simulate the process of whale predation, and the equation can be represented as:

$$\vec{X}(t+1) = \vec{X}_p(t) - \vec{A} \cdot \left| \vec{C} \cdot \vec{X}_p(t) - \vec{X}(t) \right| \tag{19}$$

where, $\vec{X}$ is the position vector of the search agent; t represents the current iteration number; $\vec{X}_p(t)$ represents the position of the optimal value (prey) under current iteration; $\vec{A} \cdot \left| \vec{C} \cdot \vec{X}_p(t) - \vec{X}(t) \right|$ represents the length of the search agent's reduction to the current optimal value, which is used to simulate the process of whale surrounding the prey; $\vec{A}$ and $\vec{C}$ are coefficient vectors used to control the indentation effect of the search agent, which are described as:

$$\vec{A} = 2\vec{a} \cdot \vec{r} - \vec{a} \tag{20}$$

$$\vec{C} = 2 \cdot \vec{r} \tag{21}$$

where, $\vec{A}$ represents the random number between [-1,1]; $\vec{a}$ is the convergence factor, which gradually decreases from 2 to 0 with the continuous search of the algorithm; $\vec{r}$ represents the random number between [0,1]. It is not difficult to see that the shrinking envelopment mechanism gradually decreases with the convergence factor $\vec{a}$ to achieve the continuous shrinking process during the predation of whales. In fact, in addition to the shrinking encirclement close to prey, whale populations also randomly look for prey based on each other's location. The equation for simulating random search of whale population is described as:

$$\vec{X}(t+1) = \vec{X}_{rand}(t) - \vec{A} \cdot \left| \vec{C} \cdot \vec{X}_{rand}(t) - \vec{X}(t) \right| \tag{22}$$

where, $\vec{A}$ have the same meaning with Eq. (19) and $\vec{X}_{rand}(t)$ represents a position vector randomly selected from the current search agent. It can be seen from Eq. (22) that the search agent can realize the process of whales randomly searching for prey by selecting random vectors. The shrinking encirclement mechanism can simulate the behavior of whale populations encircling prey and randomly searching for prey. In order to realize this mathematical model, the shrinking encircling mechanism shown in Fig. 6 [25] guides the search mode of the search agent through the coefficient vector $\vec{A}$, where (x, y) represents the location of the current search agent, and (x^*, y^*) represents the location of the current optimal value. Fig. 4 shows that the coefficient vector $\vec{A}$ can guide the search agent to realize the exploitation or exploration process. When $|\vec{A}| \le 1$, the search agent can move closer to the current optimal value, which reflects the local exploitation capability of the algorithm; when $|\vec{A}| > 1$, the search agent can randomly search areas other than the current best quality, which reflects the algorithm's global exploration capabilities. The shrinking encirclement mechanism closes or spreads to the optimal value area, so that the algorithm balances the local exploitation and global exploration. It can be seen from Eq. (18) that in addition to the shrinking encirclement mechanism, another mathematical model of WOA is the spiral update mechanism. The following Eq. (23) can express the spiral update mechanism.

$$\vec{X}(t+1) = \vec{D} \cdot e^{bl} \cdot \cos(2\pi l) + \vec{X}_P(t) \tag{23}$$

where, b is a constant used to limit the shape of the logarithmic spiral; l is a random number between [-1, 1] used to control the indentation effect of the search agent. $\vec{D}$ shown in Eq. (24) represents the distance between the i -th search agent whale and the current optimal value.

$$\vec{D} = \vec{X}_P(t) - \vec{X}(t) \tag{24}$$

The spiral updating mechanism model is shown in Fig. 5, which first calculates the distance between the search agent and the current optimal value [25]. Then, a spiral contraction route is created between them so that the search agent can achieve the current optimal value. In addition, Fig. 5 also shows the influence of parameter l on the indentation effect of the search agent.

The reduction of parameter l can enhance the indentation effect of the search agent to the current optimal value and increase the local search ability of the algorithm. The increase of parameter l can weaken the indentation effect of the search agent to the current optimal value and reduce the probability of the algorithm falling into the local optimal value. The pseudo code of WOA procedure is described as follows.

Initialize the whales population $X_i(i=1,2,3...n)$
Calculate the fitness of each search agent
X_p =the best search agent
t=1
While (t<maximum number of iterations)
For each search agent
Update a, A, C, l, and p
If (p<0.5)

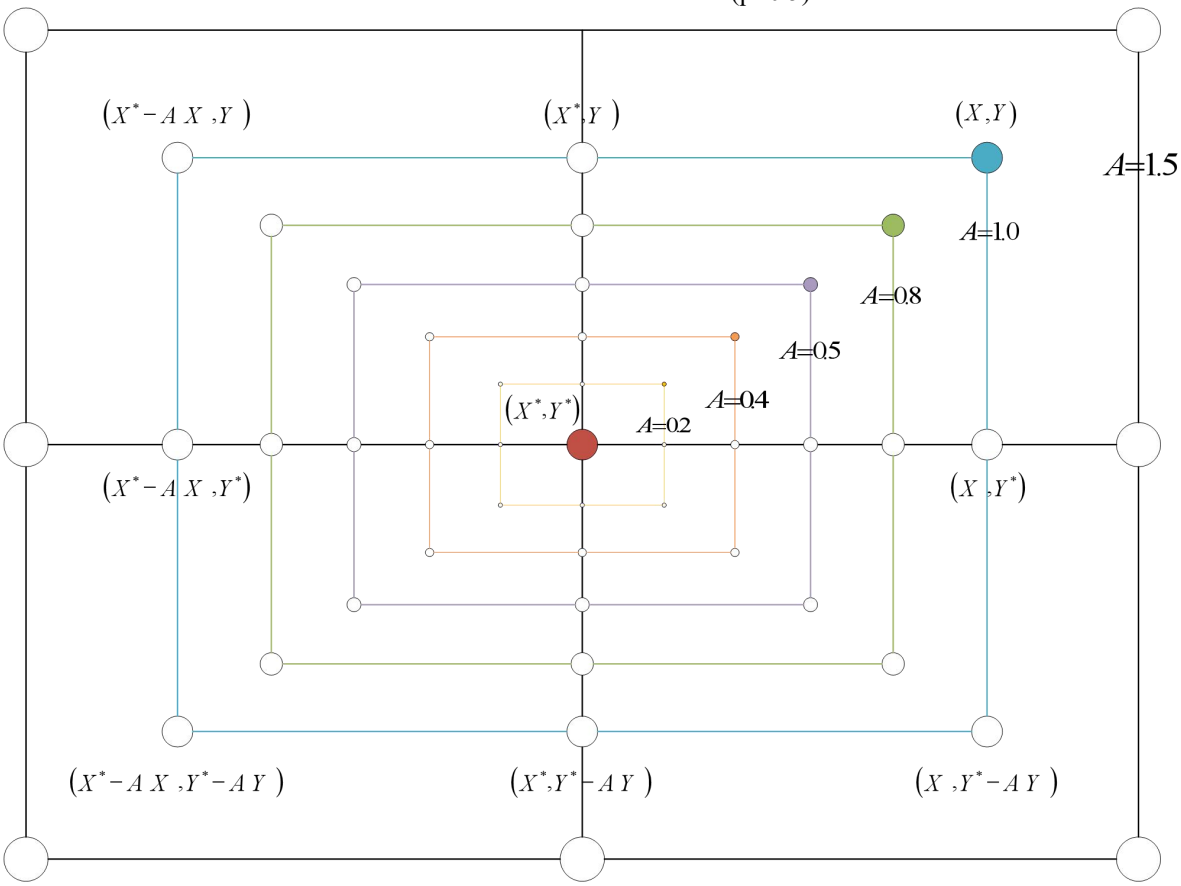

Fig. 4 Shrinkage enveloping mechanism model.

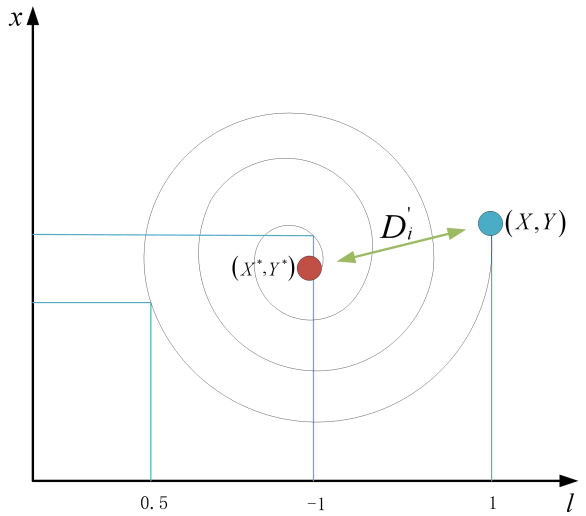

Fig. 5 Spiral update mechanism model.

If ($|A|<1$)
Update the position of search agent by the Eq.(18)
Else If ($|A|\geq 1$)
Update the position of search agent by the Eq.(20)
End If
Else If (p>0.5)
Update the position of the search agent by the Eq.(23)
End If
End For
Check if any search agent goes beyond the search space and amend it
Update X_p if there is a better solution
t=t+1
End While
Return X_p

C. WOA-MLSVMs Identification Method of Banknotes Dirty Degree

The banknotes dirty image recognition is a multi-classification problem, and the traditional SVM is only suitable for two classification problems. At present, SVM mainly deals with multiple classification problems including "One-Versus-All"(OVA), "One-Versus-the-Rest" (OVR) and hierarchical classification. The OVA classification method adopted in this paper is aimed at the l -class classification problem. It is necessary to construct l class SVM classifiers. The i -th SVM classifier marks the samples in the i -th class as +1, and the other samples as −1, thus separating each class from other classes, that is to say that the classification hyperplane constructed by the i -th classifier separates the i -th class from the other $i-1$ classes.

In their research, Vapnik et al. found that the RBF parameter γ and the error penalty factor C are the key factors affecting the performance of SVM [22]. The kernel function parameter γ mainly affects the complexity of the distribution of sample data in the high-dimensional feature space, and the error penalty factor C is used to adjust the confidence range of the learning machine and the ratio of experience risk in the determined feature space. In this paper, WOA is used to optimize the parameters γ and C of the MLSVMs to improve the recognition accuracy of banknotes dirty degree. Since the goal of WOA is to optimize the parameters of MLSVMs so as to improve the classification accuracy, that is, the higher the classification accuracy that an individual can produce by the classifier, the higher its fitness value should be. The banknotes dirty degree recognition data set is divided into two parts. One part is used to train MLSVMs and the other part is used to test the model to obtain the individual fitness value.

$$Fitness = \sum_{i=1}^{V_{size}} M_i \Big/ V_{size} \tag{25}$$

where, V_{size} is the size of the test set; M_i is the match between the classification result and the actual result. When the classification result is the same as the actual result, M_i is 1; otherwise, it is 0. It can be said that $Fitness$ is the average classification accuracy of SVM model.

The algorithm flowchart of optimizing MLSVMs model parameters γ and C based on WOA mainly follows the program pseudo code described in the previous section. Real-number encoding method is performed on the Gaussian radial basis kernel function parameter γ and error penalty factor C , the intelligent search population is randomly initialized in the searching space, and each search agent is used as the kernel function parameter γ and error penalty factor C of MLSVMs in turn. Then use the training data set to trained it and the test data set is identified. The fitness values are calculated according to the correct recognition rate shown in Eq. (25). Finally, WOA is used to iteratively optimize these two parameters and the optimal penalty factor C and the kernel function parameter γ are used as the parameters of MLSVMs to realize the recognition of banknotes dirty degree.

V. Simulation Experiments and Result Analysis

This article divides the 1000 banknotes into five categories according to their dirty degree: New, Clean, Normal, Dirty, and Very dirty, whose number are 272 banknotes, 200 sheets, 220 sheets, 170 sheets and 138 sheets. Each image resolution is 600 × 288 pixels. For 10 banknotes double-sided reflection images under red light, green light, blue light, infrared light and ultraviolet light, and 2 banknotes images under green light transmission and infrared light transmission, 22 texture feature parameters such as angular second moment, entropy, dissimilarity and contrast based on gray-level co-occurrence matrix are used to describe the dirty degree of banknotes. The correlation dimension estimator, geodesic minimum spanning tree algorithm, principal component analysis method, and maximum likelihood estimator are used to estimate the essential dimension. The essential dimension estimation results of the high-dimensional data with 176-dimensional texture features under full-spectrum are respectively 2, 9, 5 and 7. Then two data dimension reduction strategies, the laplacian eigenmaps (Laplacian) and t-distributed stochastic neighbor embedding (tSNE), are used to reduce the dimension of the 176-dimensional texture feature high-dimensional data under full spectrum. The dimension reduced data are used as the simulation research data in this section. Then the data after dimension reduction is normalized and divided into two parts. The last 20 sets of data for each type of banknotes are used as test sample data to verify the performance of the banknotes dirty degree recognition model, and other data are used as the training data for MLSVMs. The parameters of whale optimization algorithm (WOA) are initialized. The number of search agents is 20, the maximum number of iterations is 100, and the search upper and lower limits of the initial penalty factor C and parameter γ are both 0.001 and 100. Under two data dimension reduction strategies of laplacian eigenmaps (Laplacian) and t-distributed stochastic neighbor embedding (tSNE), the final optimization parameters of multi-layer support vector machines (WOA-MLSVMs) based on the whale optimization algorithm are shown in Table 5. The banknotes dirty degree recognition results based on MLSVMs and WOA-MLSVMs models are shown in Fig. 6 and Table 6.

It can be seen from Table 5 that based on two dimension reduction methods of laplacian eigenmaps (Laplacian) and t-distributed stochastic neighbor embedding (tSNE), when the intrinsic dimensions are 2, 5, 7 and 9, the gaussian radial basis kernel function parameter γ and error penalty factor C in MLSVMs optimized by WOA are different, but the recognition accuracy based on the optimized γ and C is more accurate than the non-optimized MLSVMs. The recognition accuracy rate has increased substantially. It can be seen from Fig. 6 and Table 6 that based on the laplacian data dimension reduction method, the MLSVMs models have the accuracy of 57%, 53%, 55% and 55% respectively under the four essential dimensions. 53%, while the dirty degree recognition accuracies of WOA-MLSVMs model are 81%, 80%, 79%, and 80% under four essential dimensions, with an increase of 24%, 27%, 24% and 27%, respectively. An increase of 25.5 percentage points is obtained in average. Based on the t-distributed stochastic neighbor embedding (tSNE) data dimension reduction method, the banknotes dirty degree recognition accuracies of MLSVMs model are 54%, 54%, 54%, and 52% under four essential dimensions.

TABLE 5 PARAMETERS OPTIMIZATION RESULTS OF WOA-MLSVMS

Dimension reduction method	Recognition method	Parameters of MLSVMs							
		Dim=2		Dim=5		Dim=7		Dim=9	
		C	γ	C	γ	C	γ	C	γ
Laplacian	WOA-MLSVMs	56.862	32.873	39.318	8.766	29.021	4.333	96.151	2.351
tSNE	WOA-MLSVMs	96.859	17.045	11.646	27.811	8.939	11.290	32.827	9.015

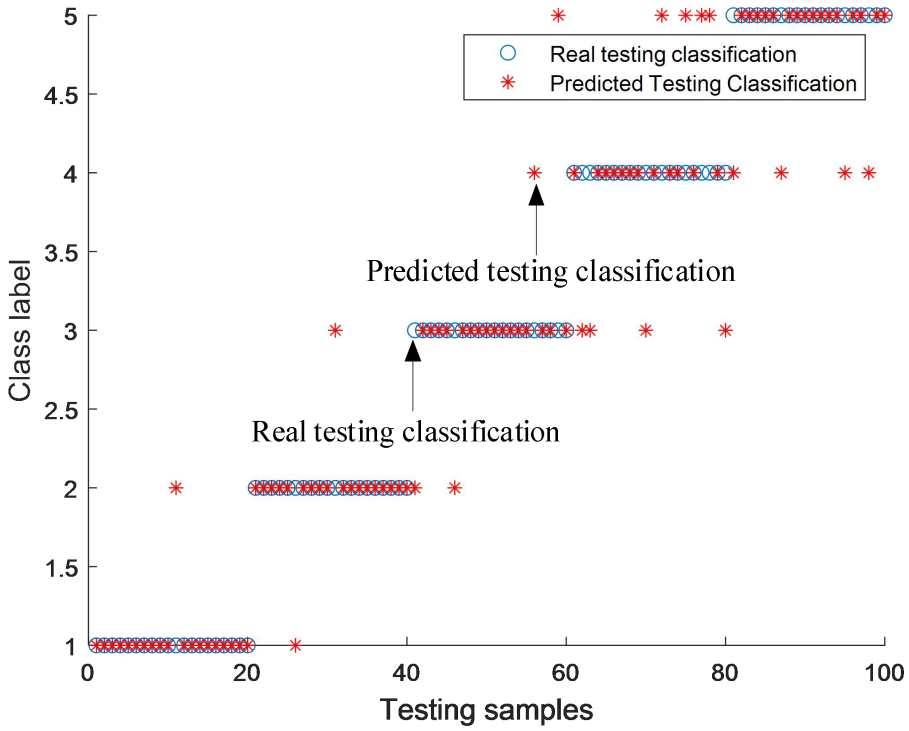

(a) Laplacian (Dim=2)

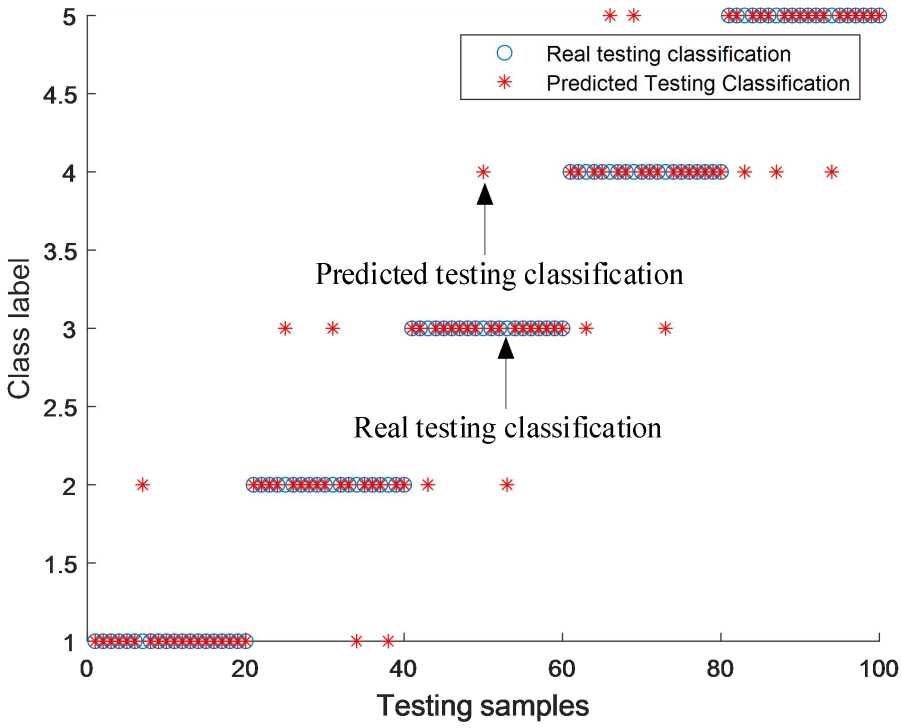

(b) tSNE (Dim=5)

Fig. 6 Recognition results of banknote dirt degree based on WOA-MLSVMs.

TABLE 6 DIRTY DEGREE RECOGNITION RESULTS OF BANKNOTES

Dimension reduction method	Recognition methods	Accuracy (%)			
		Dim=2	Dim=5	Dim=7	Dim=9
Laplacian	MLSVMs	57	53	55	53
	WOA-MLSVMs	**81**	80	79	80
tSNE	MLSVMs	54	54	54	52
	WOA-MLSVMs	80	**85**	84	82

The WOA-MLSVMs model has 80%, 85%, 84%, and 82% accuracy in the dirty degree recognition rata under four essential dimensions, which are improved by 26%, 31%, 30%, and 30%, respectively, and an average increase of 29.25 percentage point. In short, the WOA-MLSVMs model based on the full-spectrum image texture characteristics of banknotes basically achieves a recognition accuracy of over 80% and the highest recognition accuracy of 85%, which basically meets the requirements of intelligent banknote sorting.

VI. CONCLUSION

This paper proposes a banknotes dirty degree recognition method based on paper currency image texture features and multi-layer support vector machines (MLSVMs). The gray co-occurrence matrix and related 22 feature parameters are used to describe the visual characteristics of the dirty degree by using the double-sided reflection images under red, green, blue, infrared and ultraviolet light, as well as green light transmission and infrared light transmission images of 1000 banknotes. Then, 5 essential dimension estimation methods and 17 data dimension reduction methods are combined to determine the essential dimension and the optimal dimension reduction method. Finally, the implementation of MLSVMs based on the whale optimization algorithm by using full-spectrum banknotes images is to realize the dirty degree recognition and the simulation experiments results show the effectiveness of the proposed method.

REFERENCES

[1] L. Ji, H. Hyung, K. Ki, and P. Kang, "A Survey on Banknote Recognition Methods by Various Sensors," *Sensors*, vol. 17, no. 2, pp. 313, 2017.

[2] Y. X. Zhang, and H. Sun, "Research on Multi-features Fusion Banknote Identification Method Based on D-S Evidence Theory," *Computer Knowledge and Technology*, vol. 14, no. 21, pp. 232-235, 2018.

[3] C. Y. Yeh, W. P. Su, and S. J. Lee, "Employing Multiple-kernel Support Vector Machines for Counterfeit Banknote Recognition," *Applied Soft Computing*, vol. 11, no. 1, pp. 1439-1447, 2011.

[4] F. Takeda, T. Nishikage, and S. Omatu, "Banknote Recognition by Means of Optimized Masks, Neural Networks and Genetic Algorithms," *Engineering Applications of Artificial Intelligence*, vol. 12, no. 2, pp. 175-184, 1999.

[5] O. K. Oyedotun, and A. Khashman, "Banknote Recognition: Investigating Processing and Cognition Framework Using Competitive Neural Network," *Cognitive Neurodynamics*, vol. 11, no. 1, pp. 1-13, 2017.

[6] T. D. Pham, Y. H. Park, S. Y. Kwon, K. R. Park, and S. Yoon, "Efficient Banknote Recognition Based on Selection of Discriminative Regions with One-Dimensional Visible-Light Line Sensor," *Pattern Recognition*, vol. 72, no. 3, pp. 27-43, 2017.

[7] Z. Lin, Z. He, P. Wang, B. Tan, and Y. Bai, "SNRNet: a Deep Learning-Based Network for Banknote Serial Number Recognition," *Neural Processing Letters*, vol. 52, no. 3, pp. 1415-1426, 2020.

[8] Y. Jin, L. Song, X. Tang, and M. Du, "A Hierarchical Approach for Banknote Image Processing Using Homogeneity and FFD Model," *IEEE Signal Processing Letters*, vol. 15, pp. 425-428, 2008.

[9] M. Han, and J. Kim, "Joint Banknote Recognition and Counterfeit Detection Using Explainable Artificial Intelligence," *Sensors*, vol. 19, no. 16, pp. 3607, 2019.

[10] E. Choi, S. Chae, and J. Kim, "Machine Learning-Based Fast Banknote Serial Number Recognition Using Knowledge Distillation and Bayesian Optimization," *Sensors*, vol. 19, no. 19, pp. 4218, 2019.

[11] T. Pham, D. Lee, and K. Park, "Multi-National Banknote Classification Based on Visible-light Line Sensor and Convolutional Neural Network," *Sensors*, vol. 17, no. 72, pp. 1595, 2017.

[12] S. Gai, "New Banknote Defect Detection Algorithm Using Quaternion Wavelet Transform," *Neurocomputing*, vol. 196, pp. 133-139, 2016.

[13] S. Gai, G. Yang, and M. Wan, "Employing Quaternion Wavelet Transform for Banknote Classification," *Neurocomputing*, vol. 118, pp. 171-178, 2013.

[14] T. Y. Kyrychok, "An Analysis of the Precision of Indicators of the General Deterioration of Banknotes," *Measurement Techniques*, vol. 57, no. 2, pp. 166-171, 2014.

[15] P. Tuyen, P. Young, K. Seung, N. Dat, V. Husan, and P. Kang, et al., "Recognizing Banknote Fitness with a Visible Light One Dimensional Line Image Sensor," *Sensors*, vol. 15, no. 9, pp. 21016-21032, 2015.

[16] K. Seung, P. Tuyen, P. Kang, J. Dae, and Y. Sungsoo, "Recognition of Banknote Fitness Based on a Fuzzy System Using Visible Light Reflection and Near-infrared Light Transmission Images," *Sensors*, vol. 16, no. 6, pp. 863, 2016.

[17] W. Z. Sun, Y. Ma, Z. Y. Yin, A. Gu, and F. L. Xu, "Banknote Dirty Identification Method Based on Convolutional Neural Network," *Journal of Chinese Computer Systems*, vol. 41, no. 7, pp. 1508-1512, 2020.

[18] J. S. Wang, and X. D. Ren, "GLCM Based Extraction of Flame Image Texture Features and KPCA-GLVQ Recognition Method for Rotary Kiln Combustion Working Conditions," *International Journal of Automation & Computing*, vol. 11, no. 1, pp. 72-77, 2014.

[19] R. Bennett, "The Intrinsic Dimensionality of Signal Collections," *IEEE Transactions on Information Theory*, vol. 15, no. 5, pp. 517-525, 1969.

[20] C. Qin, S. Song, G. Huang, and L. Zhu, "Unsupervised Neighborhood Component Analysis for Clustering," *Neurocomputing*, vol. 168, pp. 609-617, 2015.

[21] W. Xie, J. S. Wang, C. Xing, S. S. Guo, M. W. Guo, and L. F. Zhu, "Adaptive Hybrid Soft-Sensor Model of Grinding Process Based on Regularized Extreme Learning Machine and Least Squares Support Vector Machine Optimized by Golden Sine Harris Hawk Optimization Algorithm," *Complexity*, vol. 2020, pp. 1-26, 2020.

[22] S. Wen, J. S. Wang, and J. Gao, "Fault Diagnosis Strategy of Polymerization Kettle Equipment Based on Support Vector Machine and Cuckoo Search Algorithm," *Engineering Letters*. vol. 25, no. 4, pp. 474-482, 2017.

[23] S. Mirjalili, and A. Lewis, "The Whale Optimization Algorithm," *Advances in engineering software*, vol. 95, pp. 51-67, 2016.

[24] W. Z. Sun, J. S. Wang, and W. Xian, "An Improved Whale Optimization Algorithm Based on Different Searching Paths and Perceptual Disturbance," *Symmetry,* vol. 10, no. 6, pp. 210, 2018.

[25] J. Zhang, and J. S. Wang," Improved Whale Optimization Algorithm Based On Nonlinear Adaptive Weight and Golden Sine Operator," *IEEE Access*, vol. 8, pp. 77013-77048, 2020.